First Observation of Heavy Baryons Σ_b and Σ_b^*

T. Aaltonen,[23] A. Abulencia,[24] J. Adelman,[13] T. Affolder,[10] T. Akimoto,[55] M.G. Albrow,[17] S. Amerio,[43] D. Amidei,[35] A. Anastassov,[52] K. Anikeev,[17] A. Annovi,[19] J. Antos,[14] M. Aoki,[55] G. Apollinari,[17] T. Arisawa,[57] A. Artikov,[15] W. Ashmanskas,[17] A. Attal,[3] A. Aurisano,[53] F. Azfar,[42] P. Azzi-Bacchetta,[43] P. Azzurri,[46] N. Bacchetta,[43] W. Badgett,[17] A. Barbaro-Galtieri,[29] V.E. Barnes,[48] B.A. Barnett,[25] S. Baroiant,[7] V. Bartsch,[31] G. Bauer,[33] P.-H. Beauchemin,[34] F. Bedeschi,[46] S. Behari,[25] G. Bellettini,[46] J. Bellinger,[59] A. Belloni,[33] D. Benjamin,[16] A. Beretvas,[17] J. Beringer,[29] T. Berry,[30] A. Bhatti,[50] M. Binkley,[17] D. Bisello,[43] I. Bizjak,[31] R.E. Blair,[2] C. Blocker,[6] B. Blumenfeld,[25] A. Bocci,[16] A. Bodek,[49] V. Boisvert,[49] G. Bolla,[48] A. Bolshov,[33] D. Bortoletto,[48] J. Boudreau,[47] A. Boveia,[10] B. Brau,[10] L. Brigliadori,[5] C. Bromberg,[36] E. Brubaker,[13] J. Budagov,[15] H.S. Budd,[49] S. Budd,[24] K. Burkett,[17] G. Busetto,[43] P. Bussey,[21] A. Buzatu,[34] K. L. Byrum,[2] S. Cabrera[q],[16] M. Campanelli,[20] M. Campbell,[35] F. Canelli,[17] A. Canepa,[45] S. Carillo[i],[18] D. Carlsmith,[59] R. Carosi,[46] S. Carron,[34] B. Casal,[11] M. Casarsa,[54] A. Castro,[5] P. Catastini,[46] D. Cauz,[54] M. Cavalli-Sforza,[3] A. Cerri,[29] L. Cerrito[m],[31] S.H. Chang,[28] Y.C. Chen,[1] M. Chertok,[7] G. Chiarelli,[46] G. Chlachidze,[17] F. Chlebana,[17] I. Cho,[28] K. Cho,[28] D. Chokheli,[15] J.P. Chou,[22] G. Choudalakis,[33] S.H. Chuang,[52] K. Chung,[12] W.H. Chung,[59] Y.S. Chung,[49] M. Cilijak,[46] C.I. Ciobanu,[24] M.A. Ciocci,[46] A. Clark,[20] D. Clark,[6] M. Coca,[16] G. Compostella,[43] M.E. Convery,[50] J. Conway,[7] B. Cooper,[31] K. Copic,[35] M. Cordelli,[19] G. Cortiana,[43] F. Crescioli,[46] C. Cuenca Almenar[q],[7] J. Cuevas[l],[11] R. Culbertson,[17] J.C. Cully,[35] S. DaRonco,[43] M. Datta,[17] S. D'Auria,[21] T. Davies,[21] D. Dagenhart,[17] P. de Barbaro,[49] S. De Cecco,[51] A. Deisher,[29] G. De Lentdecker[c],[49] G. De Lorenzo,[3] M. Dell'Orso,[46] F. Delli Paoli,[43] L. Demortier,[50] J. Deng,[16] M. Deninno,[5] D. De Pedis,[51] P.F. Derwent,[17] G.P. Di Giovanni,[44] C. Dionisi,[51] B. Di Ruzza,[54] J.R. Dittmann,[4] M. D'Onofrio,[3] C. Dörr,[26] S. Donati,[46] P. Dong,[8] J. Donini,[43] T. Dorigo,[43] S. Dube,[52] J. Efron,[39] R. Erbacher,[7] D. Errede,[24] S. Errede,[24] R. Eusebi,[17] H.C. Fang,[29] S. Farrington,[30] I. Fedorko,[46] W.T. Fedorko,[13] R.G. Feild,[60] M. Feindt,[26] J.P. Fernandez,[32] R. Field,[18] G. Flanagan,[48] R. Forrest,[7] S. Forrester,[7] M. Franklin,[22] J.C. Freeman,[29] I. Furic,[13] M. Gallinaro,[50] J. Galyardt,[12] J.E. Garcia,[46] F. Garberson,[10] A.F. Garfinkel,[48] C. Gay,[60] H. Gerberich,[24] D. Gerdes,[35] S. Giagu,[51] P. Giannetti,[46] K. Gibson,[47] J.L. Gimmell,[49] C. Ginsburg,[17] N. Giokaris[a],[15] M. Giordani,[54] P. Giromini,[19] M. Giunta,[46] G. Giurgiu,[25] V. Glagolev,[15] D. Glenzinski,[17] M. Gold,[37] N. Goldschmidt,[18] J. Goldstein[b],[42] A. Golossanov,[17] G. Gomez,[11] G. Gomez-Ceballos,[33] M. Goncharov,[53] O. González,[32] I. Gorelov,[37] A.T. Goshaw,[16] K. Goulianos,[50] A. Gresele,[43] S. Grinstein,[22] C. Grosso-Pilcher,[13] R.C. Group,[17] U. Grundler,[24] J. Guimaraes da Costa,[22] Z. Gunay-Unalan,[36] C. Haber,[29] K. Hahn,[33] S.R. Hahn,[17] E. Halkiadakis,[52] A. Hamilton,[20] B.-Y. Han,[49] J.Y. Han,[49] R. Handler,[59] F. Happacher,[19] K. Hara,[55] D. Hare,[52] M. Hare,[56] S. Harper,[42] R.F. Harr,[58] R.M. Harris,[17] M. Hartz,[47] K. Hatakeyama,[50] J. Hauser,[8] C. Hays,[42] M. Heck,[26] A. Heijboer,[45] B. Heinemann,[29] J. Heinrich,[45] C. Henderson,[33] M. Herndon,[59] J. Heuser,[26] D. Hidas,[16] C.S. Hill[b],[10] D. Hirschbuehl,[26] A. Hocker,[17] A. Holloway,[22] S. Hou,[1] M. Houlden,[30] S.-C. Hsu,[9] B.T. Huffman,[42] R.E. Hughes,[39] U. Husemann,[60] J. Huston,[36] J. Incandela,[10] G. Introzzi,[46] M. Iori,[51] A. Ivanov,[7] B. Iyutin,[33] E. James,[17] D. Jang,[52] B. Jayatilaka,[16] D. Jeans,[51] E.J. Jeon,[28] S. Jindariani,[18] W. Johnson,[7] M. Jones,[48] K.K. Joo,[28] S.Y. Jun,[12] J.E. Jung,[28] T.R. Junk,[24] T. Kamon,[53] P.E. Karchin,[58] Y. Kato,[41] Y. Kemp,[26] R. Kephart,[17] U. Kerzel,[26] V. Khotilovich,[53] B. Kilminster,[39] D.H. Kim,[28] H.S. Kim,[28] J.E. Kim,[28] M.J. Kim,[17] S.B. Kim,[28] S.H. Kim,[55] Y.K. Kim,[13] N. Kimura,[55] L. Kirsch,[6] S. Klimenko,[18] M. Klute,[33] B. Knuteson,[33] B.R. Ko,[16] K. Kondo,[57] D.J. Kong,[28] J. Konigsberg,[18] A. Korytov,[18] A.V. Kotwal,[16] A.C. Kraan,[45] J. Kraus,[24] M. Kreps,[26] J. Kroll,[45] N. Krumnack,[4] M. Kruse,[16] V. Krutelyov,[10] T. Kubo,[55] S. E. Kuhlmann,[2] T. Kuhr,[26] N.P. Kulkarni,[58] Y. Kusakabe,[57] S. Kwang,[13] A.T. Laasanen,[48] S. Lai,[34] S. Lami,[46] S. Lammel,[17] M. Lancaster,[31] R.L. Lander,[7] K. Lannon,[39] A. Lath,[52] G. Latino,[46] I. Lazzizzera,[43] T. LeCompte,[2] J. Lee,[49] J. Lee,[28] Y.J. Lee,[28] S.W. Lee[o],[53] R. Lefèvre,[20] N. Leonardo,[33] S. Leone,[46] S. Levy,[13] J.D. Lewis,[17] C. Lin,[60] C.S. Lin,[17] M. Lindgren,[17] E. Lipeles,[9] A. Lister,[7] D.O. Litvintsev,[17] T. Liu,[17] N.S. Lockyer,[45] A. Loginov,[60] M. Loreti,[43] R.-S. Lu,[1] D. Lucchesi,[43] P. Lujan,[29] P. Lukens,[17] G. Lungu,[18] L. Lyons,[42] J. Lys,[29] R. Lysak,[14] E. Lytken,[48] P. Mack,[26] D. MacQueen,[34] R. Madrak,[17] K. Maeshima,[17] K. Makhoul,[33] T. Maki,[23] P. Maksimovic,[25] S. Malde,[42] S. Malik,[31] G. Manca,[30] A. Manousakis[a],[15] F. Margaroli,[5] R. Marginean,[17] C. Marino,[26] C.P. Marino,[24] A. Martin,[60] M. Martin,[25] V. Martin[g],[21] M. Martínez,[3] R. Martínez-Ballarín,[32] T. Maruyama,[55] P. Mastrandrea,[51] T. Masubuchi,[55] H. Matsunaga,[55] M.E. Mattson,[58] R. Mazini,[34] P. Mazzanti,[5] K.S. McFarland,[49] P. McIntyre,[53] R. McNulty[f],[30] A. Mehta,[30] P. Mehtala,[23] S. Menzemer[h],[11] A. Menzione,[46] P. Merkel,[48] C. Mesropian,[50] A. Messina,[36] T. Miao,[17] N. Miladinovic,[6] J. Miles,[33] R. Miller,[36] C. Mills,[10] M. Milnik,[26] A. Mitra,[1] G. Mitselmakher,[18] A. Miyamoto,[27]

S. Moed,[20] N. Moggi,[5] B. Mohr,[8] C.S. Moon,[28] R. Moore,[17] M. Morello,[46] P. Movilla Fernandez,[29] J. Mülmenstädt,[29] A. Mukherjee,[17] Th. Muller,[26] R. Mumford,[25] P. Murat,[17] M. Mussini,[5] J. Nachtman,[17] A. Nagano,[55] J. Naganoma,[57] K. Nakamura,[55] I. Nakano,[40] A. Napier,[56] V. Necula,[16] C. Neu,[45] M.S. Neubauer,[9] J. Nielsen[n],[29] L. Nodulman,[2] O. Norniella,[3] E. Nurse,[31] S.H. Oh,[16] Y.D. Oh,[28] I. Oksuzian,[18] T. Okusawa,[41] R. Oldeman,[30] R. Orava,[23] K. Osterberg,[23] C. Pagliarone,[46] E. Palencia,[11] V. Papadimitriou,[17] A. Papaikonomou,[26] A.A. Paramonov,[13] B. Parks,[39] S. Pashapour,[34] J. Patrick,[17] G. Pauletta,[54] M. Paulini,[12] C. Paus,[33] D.E. Pellett,[7] A. Penzo,[54] T.J. Phillips,[16] G. Piacentino,[46] J. Piedra,[44] L. Pinera,[18] K. Pitts,[24] C. Plager,[8] L. Pondrom,[59] X. Portell,[3] O. Poukhov,[15] N. Pounder,[42] F. Prakoshyn,[15] A. Pronko,[17] J. Proudfoot,[2] F. Ptohos[e],[19] G. Punzi,[46] J. Pursley,[25] J. Rademacker[b],[42] A. Rahaman,[47] V. Ramakrishnan,[59] N. Ranjan,[48] I. Redondo,[32] B. Reisert,[17] V. Rekovic,[37] P. Renton,[42] M. Rescigno,[51] S. Richter,[26] F. Rimondi,[5] L. Ristori,[46] A. Robson,[21] T. Rodrigo,[11] E. Rogers,[24] S. Rolli,[56] R. Roser,[17] M. Rossi,[54] R. Rossin,[10] P. Roy,[34] A. Ruiz,[11] J. Russ,[12] V. Rusu,[13] H. Saarikko,[23] A. Safonov,[53] W.K. Sakumoto,[49] G. Salamanna,[51] O. Saltó,[3] L. Santi,[54] S. Sarkar,[51] L. Sartori,[46] K. Sato,[17] P. Savard,[34] A. Savoy-Navarro,[44] T. Scheidle,[26] P. Schlabach,[17] E.E. Schmidt,[17] M.A. Schmidt,[13] M.P. Schmidt,[60] M. Schmitt,[38] T. Schwarz,[7] L. Scodellaro,[11] A.L. Scott,[10] A. Scribano,[46] F. Scuri,[46] A. Sedov,[48] S. Seidel,[37] Y. Seiya,[41] A. Semenov,[15] L. Sexton-Kennedy,[17] A. Sfyrla,[20] S.Z. Shalhout,[58] M.D. Shapiro,[29] T. Shears,[30] P.F. Shepard,[47] D. Sherman,[22] M. Shimojima[k],[55] M. Shochet,[13] Y. Shon,[59] I. Shreyber,[20] A. Sidoti,[46] P. Sinervo,[34] A. Sisakyan,[15] A.J. Slaughter,[17] J. Slaunwhite,[39] K. Sliwa,[56] J.R. Smith,[7] F.D. Snider,[17] R. Snihur,[34] M. Soderberg,[35] A. Soha,[7] S. Somalwar,[52] V. Sorin,[36] J. Spalding,[17] F. Spinella,[46] T. Spreitzer,[34] P. Squillacioti,[46] M. Stanitzki,[60] A. Staveris-Polykalas,[46] R. St. Denis,[21] B. Stelzer,[8] O. Stelzer-Chilton,[42] D. Stentz,[38] J. Strologas,[37] D. Stuart,[10] J.S. Suh,[28] A. Sukhanov,[18] H. Sun,[56] I. Suslov,[15] T. Suzuki,[55] A. Taffard[p],[24] R. Takashima,[40] Y. Takeuchi,[55] R. Tanaka,[40] M. Tecchio,[35] P.K. Teng,[1] K. Terashi,[50] R.J. Tesarek,[17] J. Thom[d],[17] A.S. Thompson,[21] E. Thomson,[45] P. Tipton,[60] V. Tiwari,[12] S. Tkaczyk,[17] D. Toback,[53] S. Tokar,[14] K. Tollefson,[36] T. Tomura,[55] D. Tonelli,[46] S. Torre,[19] D. Torretta,[17] S. Tourneur,[44] W. Trischuk,[34] S. Tsuno,[40] Y. Tu,[45] N. Turini,[46] F. Ukegawa,[55] S. Uozumi,[55] S. Vallecorsa,[20] N. van Remortel,[23] A. Varganov,[35] E. Vataga,[37] F. Vazquez[i],[18] G. Velev,[17] C. Vellidis[a],[46] G. Veramendi,[24] V. Veszpremi,[48] M. Vidal,[32] R. Vidal,[17] I. Vila,[11] R. Vilar,[11] T. Vine,[31] M. Vogel,[37] I. Vollrath,[34] I. Volobouev[o],[29] G. Volpi,[46] F. Würthwein,[9] P. Wagner,[53] R.G. Wagner,[2] R.L. Wagner,[17] J. Wagner,[26] W. Wagner,[26] R. Wallny,[8] S.M. Wang,[1] A. Warburton,[34] D. Waters,[31] M. Weinberger,[53] W.C. Wester III,[17] B. Whitehouse,[56] D. Whiteson,[45] A.B. Wicklund,[2] E. Wicklund,[17] G. Williams,[34] H.H. Williams,[45] P. Wilson,[17] B.L. Winer,[39] P. Wittich[d],[17] S. Wolbers,[17] C. Wolfe,[13] T. Wright,[35] X. Wu,[20] S.M. Wynne,[30] A. Yagil,[9] K. Yamamoto,[41] J. Yamaoka,[52] T. Yamashita,[40] C. Yang,[60] U.K. Yang[j],[13] Y.C. Yang,[28] W.M. Yao,[29] G.P. Yeh,[17] J. Yoh,[17] K. Yorita,[13] T. Yoshida,[41] G.B. Yu,[49] I. Yu,[28] S.S. Yu,[17] J.C. Yun,[17] L. Zanello,[51] A. Zanetti,[54] I. Zaw,[22] X. Zhang,[24] J. Zhou,[52] and S. Zucchelli[5]

(CDF Collaboration*)

[1]*Institute of Physics, Academia Sinica, Taipei, Taiwan 11529, Republic of China*
[2]*Argonne National Laboratory, Argonne, Illinois 60439*
[3]*Institut de Fisica d'Altes Energies, Universitat Autonoma de Barcelona, E-08193, Bellaterra (Barcelona), Spain*
[4]*Baylor University, Waco, Texas 76798*
[5]*Istituto Nazionale di Fisica Nucleare, University of Bologna, I-40127 Bologna, Italy*
[6]*Brandeis University, Waltham, Massachusetts 02254*
[7]*University of California, Davis, Davis, California 95616*
[8]*University of California, Los Angeles, Los Angeles, California 90024*
[9]*University of California, San Diego, La Jolla, California 92093*
[10]*University of California, Santa Barbara, Santa Barbara, California 93106*
[11]*Instituto de Fisica de Cantabria, CSIC-University of Cantabria, 39005 Santander, Spain*
[12]*Carnegie Mellon University, Pittsburgh, PA 15213*
[13]*Enrico Fermi Institute, University of Chicago, Chicago, Illinois 60637*
[14]*Comenius University, 842 48 Bratislava, Slovakia; Institute of Experimental Physics, 040 01 Kosice, Slovakia*
[15]*Joint Institute for Nuclear Research, RU-141980 Dubna, Russia*
[16]*Duke University, Durham, North Carolina 27708*
[17]*Fermi National Accelerator Laboratory, Batavia, Illinois 60510*
[18]*University of Florida, Gainesville, Florida 32611*
[19]*Laboratori Nazionali di Frascati, Istituto Nazionale di Fisica Nucleare, I-00044 Frascati, Italy*
[20]*University of Geneva, CH-1211 Geneva 4, Switzerland*
[21]*Glasgow University, Glasgow G12 8QQ, United Kingdom*
[22]*Harvard University, Cambridge, Massachusetts 02138*

[23]Division of High Energy Physics, Department of Physics, University of Helsinki and Helsinki Institute of Physics, FIN-00014, Helsinki, Finland
[24]University of Illinois, Urbana, Illinois 61801
[25]The Johns Hopkins University, Baltimore, Maryland 21218
[26]Institut für Experimentelle Kernphysik, Universität Karlsruhe, 76128 Karlsruhe, Germany
[27]High Energy Accelerator Research Organization (KEK), Tsukuba, Ibaraki 305, Japan
[28]Center for High Energy Physics: Kyungpook National University, Taegu 702-701, Korea; Seoul National University, Seoul 151-742, Korea; SungKyunKwan University, Suwon 440-746, Korea
[29]Ernest Orlando Lawrence Berkeley National Laboratory, Berkeley, California 94720
[30]University of Liverpool, Liverpool L69 7ZE, United Kingdom
[31]University College London, London WC1E 6BT, United Kingdom
[32]Centro de Investigaciones Energeticas Medioambientales y Tecnologicas, E-28040 Madrid, Spain
[33]Massachusetts Institute of Technology, Cambridge, Massachusetts 02139
[34]Institute of Particle Physics: McGill University, Montréal, Canada H3A 2T8; and University of Toronto, Toronto, Canada M5S 1A7
[35]University of Michigan, Ann Arbor, Michigan 48109
[36]Michigan State University, East Lansing, Michigan 48824
[37]University of New Mexico, Albuquerque, New Mexico 87131
[38]Northwestern University, Evanston, Illinois 60208
[39]The Ohio State University, Columbus, Ohio 43210
[40]Okayama University, Okayama 700-8530, Japan
[41]Osaka City University, Osaka 588, Japan
[42]University of Oxford, Oxford OX1 3RH, United Kingdom
[43]University of Padova, Istituto Nazionale di Fisica Nucleare, Sezione di Padova-Trento, I-35131 Padova, Italy
[44]LPNHE, Universite Pierre et Marie Curie/IN2P3-CNRS, UMR7585, Paris, F-75252 France
[45]University of Pennsylvania, Philadelphia, Pennsylvania 19104
[46]Istituto Nazionale di Fisica Nucleare Pisa, Universities of Pisa, Siena and Scuola Normale Superiore, I-56127 Pisa, Italy
[47]University of Pittsburgh, Pittsburgh, Pennsylvania 15260
[48]Purdue University, West Lafayette, Indiana 47907
[49]University of Rochester, Rochester, New York 14627
[50]The Rockefeller University, New York, New York 10021
[51]Istituto Nazionale di Fisica Nucleare, Sezione di Roma 1, University of Rome "La Sapienza," I-00185 Roma, Italy
[52]Rutgers University, Piscataway, New Jersey 08855
[53]Texas A&M University, College Station, Texas 77843
[54]Istituto Nazionale di Fisica Nucleare, University of Trieste/ Udine, Italy
[55]University of Tsukuba, Tsukuba, Ibaraki 305, Japan
[56]Tufts University, Medford, Massachusetts 02155
[57]Waseda University, Tokyo 169, Japan
[58]Wayne State University, Detroit, Michigan 48201
[59]University of Wisconsin, Madison, Wisconsin 53706
[60]Yale University, New Haven, Connecticut 06520

We report an observation of new bottom baryons produced in $p\bar{p}$ collisions at the Tevatron. Using 1.1 fb^{-1} of data collected by the CDF II detector, we observe four $\Lambda_b^0\pi^\pm$ resonances in the fully reconstructed decay mode $\Lambda_b^0 \to \Lambda_c^+\pi^-$, where $\Lambda_c^+ \to pK^-\pi^+$. We interpret these states as the $\Sigma_b^{(*)\pm}$ baryons and measure their masses to be:

$$m_{\Sigma_b^+} = 5807.8^{+2.0}_{-2.2}\ (\text{stat.}) \pm 1.7\ (\text{syst.})\ \text{MeV/c}^2 \quad m_{\Sigma_b^{*+}} = 5829.0^{+1.6}_{-1.8}\ (\text{stat.})^{+1.7}_{-1.8}\ (\text{syst.})\ \text{MeV/c}^2$$
$$m_{\Sigma_b^-} = 5815.2 \pm 1.0\ (\text{stat.}) \pm 1.7\ (\text{syst.})\ \text{MeV/c}^2 \quad m_{\Sigma_b^{*-}} = 5836.4 \pm 2.0\ (\text{stat.})^{+1.8}_{-1.7}\ (\text{syst.})\ \text{MeV/c}^2$$

PACS numbers: 14.20.Mr, 13.30.Eg

*With visitors from [a]University of Athens, 15784 Athens, Greece, [b]University of Bristol, Bristol BS8 1TL, United Kingdom, [c]University Libre de Bruxelles, B-1050 Brussels, Belgium, [d]Cornell University, Ithaca, NY 14853, [e]University of Cyprus, Nicosia CY-1678, Cyprus, [f]University College Dublin, Dublin 4, Ireland, [g]University of Edinburgh, Edinburgh EH9 3JZ, United King-

Recently the CDF II detector at the Fermilab Tevatron has accumulated the world's largest sample of fully reconstructed Λ_b^0 baryons, which consist of the u, d, and b quarks, with 3180 ± 60 (stat.) $\Lambda_b^0 \to \Lambda_c^+\pi^-$ candidates. This is made possible by the large $b\bar{b}$ production cross-section in $p\bar{p}$ collisions at $\sqrt{s} = 1.96$ TeV and the ability of the CDF II experiment to select fully hadronic decays of b hadrons with a specialized trigger system. In this Letter, we present an observation of four $\Lambda_b^0\pi^\pm$ resonances, where $\Lambda_b^0 \to \Lambda_c^+\pi^-$ and $\Lambda_c^+ \to pK^-\pi^+$, using 1.1 fb^{-1} of data. The $\Lambda_b^0\pi$ states are interpreted as the lowest-lying charged Σ_b baryons and will be labeled $\Sigma_b^{(*)}$. The symbol Σ_b refers to $\Sigma_b^\pm$, while Σ_b^* refers to $\Sigma_b^{*\pm}$. Unless otherwise noted, any reference to a specific charge state implies the antiparticle state as well.

The $\Sigma_b^{(*)+}$ baryons contain one b and two u quarks, while the $\Sigma_b^{(*)-}$ baryons contain one b and two d quarks; these states are expected to exist but have not been observed. Baryons containing one bottom quark and two light quarks can be described by heavy quark effective theory (HQET) [1]. In HQET a bottom baryon consists of a b quark acting as a static source of the color field surrounded by a diquark system comprised of the two light quarks. In the lowest-lying $\Sigma_b^{(*)}$ states, the diquark system has strong isospin $I = 1$ and $J^P = 1^+$, which couples to the heavy quark spin and results in a doublet of baryons with $J^P = \frac{1}{2}^+$ (Σ_b) and $J^P = \frac{3}{2}^+$ (Σ_b^*). This doublet is degenerate for infinite b quark mass. As the b quark mass is finite, there is a hyperfine mass splitting between the $\frac{3}{2}^+$ and $\frac{1}{2}^+$ states. There is also an isospin mass splitting between the $\Sigma_b^{(*)-}$ and $\Sigma_b^{(*)+}$ states.

There exists a variety of predictions for the $\Sigma_b^{(*)}$ masses from non-relativistic and relativistic potential quark models [2], 1/N$_c$ expansion [3], quark models in the HQET approximation [4], sum rules [5], and lattice quantum chromodynamics calculations [6]. On the basis of [2–6], we expect $m(\Sigma_b) - m(\Lambda_b^0) \sim 180 - 210$ MeV/c^2, $m(\Sigma_b^*) - m(\Sigma_b) \sim 10 - 40$ MeV/c^2, and $m(\Sigma_b^{(*)-}) - m(\Sigma_b^{(*)+}) \sim 5 - 7$ MeV/c^2. The difference between the isospin mass splittings of the Σ_b^* and Σ_b multiplets is predicted to be $[m(\Sigma_b^{*+}) - m(\Sigma_b^{*-})] - [m(\Sigma_b^+) - m(\Sigma_b^-)] = 0.40 \pm 0.07$ MeV/c^2 [7]. The natural width of $\Sigma_b^{(*)}$ baryons is expected to be dominated by the P-wave one pion transition $\Sigma_b^{(*)} \to \Lambda_b^0\pi$, whose partial width depends on the available phase space and the pion coupling to a constituent quark. For the range of predicted $\Sigma_b^{(*)}$ masses, the natural widths $\Gamma(\Sigma_b^{(*)})$ calculated from an HQET prediction vary between 2 and 20 MeV/c^2 [8].

The CDF II detector is described in detail elsewhere [9]. Its components and capabilities most relevant to this analysis are the tracking system and the ability to select displaced tracks from heavy flavor decays. The tracking system lies within a uniform axial magnetic field of 1.4 T. The inner tracking volume, with radii between 2.5 and 28 cm from the beam line, is occupied by a system of double-sided silicon microstrip detectors [10]. An additional layer of single-sided silicon microstrip detectors is mounted directly on the beampipe at an average radius of 1.5 cm. The remainder of the tracking volume is occupied by a cylindrical drift chamber [11], with a radial extent of 40 to 137 cm.

A displaced track trigger is employed to select bottom and charmed hadrons [12]. This trigger requires a pair of tracks with opposite charge, identified in the transverse view [13]. The tracks must have impact parameters d_0 which fall within the range $|d_0| \in [0.12, 1.00]$ mm, where d_0 is defined as the distance of closest approach of the track to the primary vertex in the transverse plane [14]. Each track is required to have transverse momentum $p_{\rm T} > 2.0$ GeV/c. The scalar sum of the tracks' transverse momenta must exceed 5.5 GeV/c and the azimuthal angle between the tracks is required to be within the range $2^\circ - 90^\circ$. In addition, the intersection point of the triggered tracks is required to have a transverse displacement of at least 200 μm with respect to the beam line.

In reconstructing the decays $\Lambda_b^0 \to \Lambda_c^+\pi^-$ and $\Lambda_c^+ \to pK^-\pi^+$, the proton from the Λ_c^+ decay and the π^- from the Λ_b^0 decay both must have $p_{\rm T} > 2$ GeV/c, while the K^- and π^+ candidates have $p_{\rm T} > 0.5$ GeV/c to ensure well-understood tracking efficiency. We also require $p_{\rm T}(p) > p_{\rm T}(\pi^+)$ to suppress Λ_c^+ combinatorial background. No particle identification is used in this analysis. All particle hypotheses consistent with the candidate decay structure are considered. In a 3-D kinematic fit, the Λ_c^+ daughter tracks are constrained to originate from a single point. The Λ_c^+ candidate is constrained to the known Λ_c^+ mass, and the Λ_c^+ momentum vector is extrapolated to intersect the π^- momentum vector to form the Λ_b^0 vertex. The probability of the 3-D Λ_b^0 kinematic vertex fit must exceed 0.1%, and the Λ_c^+ and Λ_b^0 must have $p_{\rm T}$ greater than 4.5 and 6.0 GeV/c, respectively. To suppress prompt backgrounds from the primary interaction, we make the following decay time requirements: $ct(\Lambda_b^0) > 250$ μm and its significance $ct(\Lambda_b^0)/\sigma_{ct} > 10$. We define $ct(\Lambda_b^0) \equiv L_{\rm xy}(\Lambda_b^0) m_{\Lambda_b^0} c / p_{\rm T}(\Lambda_b^0)$ as the Λ_b^0 proper time, where $L_{\rm xy}(\Lambda_b^0)$ is defined as the length of the projection, onto the two-track momentum vector, of the transverse plane vector from the primary vertex

dom, [h]University of Heidelberg, D-69120 Heidelberg, Germany, [i]Universidad Iberoamericana, Mexico D.F., Mexico, [j]University of Manchester, Manchester M13 9PL, England, [k]Nagasaki Institute of Applied Science, Nagasaki, Japan, [l]University de Oviedo, E-33007 Oviedo, Spain, [m]University of London, Queen Mary College, London, E1 4NS, England, [n]University of California Santa Cruz, Santa Cruz, CA 95064, [o]Texas Tech University, Lubbock, TX 79409, [p]University of California, Irvine, Irvine, CA 92697, [q]IFIC(CSIC-Universitat de Valencia), 46071 Valencia, Spain,

to the Λ_b^0 vertex. We use a primary vertex determined event-by-event when computing this vertex displacement. To reduce combinatorial backgrounds and partially reconstructed decays, we also require $\left|d_0(\Lambda_b^0)\right| < 80$ μm, where $d_0(\Lambda_b^0)$ is the impact parameter of the Λ_b^0 candidate. To suppress the contributions from $\bar{B}^0 \to D^+\pi^-$ decays, where $D^+ \to K^-\pi^+\pi^+$, we require $m(pK^-\pi^+)$ to be within 16 MeV/c^2 of the known Λ_c^+ mass [15], and $ct(\Lambda_c^+) \in [-70, 200]$ μm. We define $ct(\Lambda_c^+) \equiv L_{\rm xy}(\Lambda_c^+) m_{\Lambda_c^+} c/p_{\rm T}(\Lambda_c^+)$ as the Λ_c^+ proper time, where $L_{\rm xy}(\Lambda_c^+)$ is defined as the length of the projection, onto the three-track momentum vector, of the transverse plane vector from the Λ_b^0 vertex to the Λ_c^+ vertex.

The invariant mass distribution of $\Lambda_c^+\pi^-$ candidates is shown in Fig. 1 overlaid with a binned maximum likelihood fit. A clear $\Lambda_b^0 \to \Lambda_c^+\pi^-$ signal is observed at the expected Λ_b^0 mass. The invariant mass distribution is described by several components: the $\Lambda_b^0 \to \Lambda_c^+\pi^-$ signal, a combinatorial background, partially and fully reconstructed B mesons which pass the $\Lambda_c^+\pi^-$ selection criteria, partially reconstructed Λ_b^0 decays, and fully reconstructed Λ_b^0 decays other than $\Lambda_c^+\pi^-$ (*e.g.* $\Lambda_b^0 \to \Lambda_c^+K^-$). The combinatorial background is modeled with an exponentially decreasing function. All other components are represented in the fit by fixed shapes derived from Monte Carlo (MC) simulations [16, 17]. Within the Λ_b^0 baryon and B meson groups of shapes, the normalizations are constrained by Gaussian terms to branching ratios that are either measured (for B meson decays) or theoretical predictions (for Λ_b^0 decays). The branching ratios of many yet-unobserved Λ_b^0 decay modes are extrapolated from $\mathcal{B}(\Lambda_b^0 \to \Lambda_c^+\pi^-)$ [18] and $\mathcal{B}(\Lambda_b^0 \to \Lambda_c^{*+}\pi^-)$ [19] using the ratios of branching ratios in analogous $\bar{B}^0$ decays [15]; factorization is assumed in two-body $b \to c$ decays of Λ_b^0. The fit to the invariant $\Lambda_c^+\pi^-$ mass distribution results in 3180 ± 60 (stat.) $\Lambda_b^0 \to \Lambda_c^+\pi^-$ candidates.

The reconstruction of $\Sigma_b^{(*)}$ proceeds by combining Λ_b^0 candidates in the Λ_b^0 signal region with all remaining high quality tracks. A pion mass hypothesis is used when computing the invariant mass of the $\Sigma_b^{(*)}$ candidate. To minimize the contribution of the mass resolution of each Λ_b^0 candidate, we search for narrow resonances in the mass difference distribution of $Q = m(\Lambda_b^0\pi) - m(\Lambda_b^0) - m_\pi$. The $\Sigma_b^{(*)}$ candidates are divided into two subsamples using the charge of the pion from $\Sigma_b^{(*)}$ decay, denoted by π_{Σ_b}: in the $\Lambda_b^0\pi^-$ subsample the π_{Σ_b} has the same charge as the pion from Λ_b^0 while in the $\Lambda_b^0\pi^+$ subsample the π_{Σ_b} has the opposite charge as the pion from Λ_b^0.

On the basis of the theoretical predictions in [2–6], the $\Sigma_b^{(*)}$ signal region is defined as $Q \in [30, 100]$ MeV/c^2. We optimize the $\Sigma_b^{(*)}$ selection criteria using the pure background sample in the upper and lower sideband regions of $Q \in [0, 30]$ MeV/c^2 and $Q \in [100, 500]$ MeV/c^2. These sideband regions are parameterized by a power law

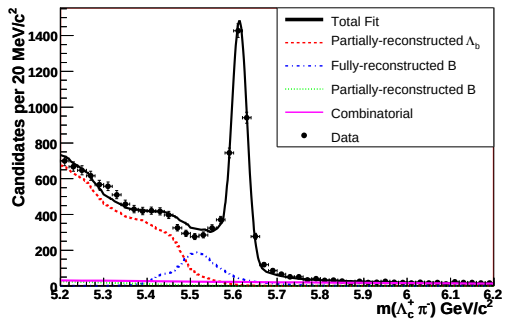

FIG. 1: Fit to the invariant mass of $\Lambda_b^0 \to \Lambda_c^+\pi^-$ candidates. Fully reconstructed Λ_b^0 decays such as $\Lambda_b^0 \to \Lambda_c^+\pi^-$ and $\Lambda_b^0 \to \Lambda_c^+K^-$ are not indicated on the figure. The Λ_b^0 signal region, $m(\Lambda_c^+\pi^-) \in [5.565, 5.670]$ GeV/c^2, consists primarily of Λ_b^0 baryons, with some contamination from B mesons and combinatorial events. The discrepancies between the fit and data below the Λ_b^0 signal region are due to incomplete knowledge of the branching ratios of the decays in this region and are included in the $\Sigma_b^{(*)}$ background model systematics.

multiplied by an exponential. The signal is modeled by the PYTHIA [20] event generator where only the decays $\Sigma_b^{(*)} \to \Lambda_b^0\pi$, $\Lambda_b^0 \to \Lambda_c^+\pi^-$, and $\Lambda_c^+ \to pK^-\pi^+$ are allowed. For the optimization, we combine the $\Lambda_b^0\pi^-$ and $\Lambda_b^0\pi^+$ subsamples. We optimize cuts on the $p_{\rm T}$ of the $\Sigma_b^{(*)}$ candidate, the impact parameter significance $|d_0/\sigma_{d_0}|$ of the π_{Σ_b} track, and the $\cos\theta^*$ of the π_{Σ_b} track, where θ^* is defined as the angle between the momentum of the π_{Σ_b} in the $\Sigma_b^{(*)}$ rest frame and the direction of the total $\Sigma_b^{(*)}$ momentum in the lab frame. The maximum of the optimization is realized for $p_{\rm T}(\Sigma_b) > 9.5$ GeV/c, $|d_0/\sigma_{d_0}| < 3.0$, and $\cos\theta^* > -0.35$.

In the $\Sigma_b^{(*)}$ search, the dominant background is from the combination of prompt Λ_b^0 baryons with extra tracks produced in the hadronization of the b quark. The remaining backgrounds are from the combination of hadronization tracks with B mesons reconstructed as Λ_b^0 baryons, and from combinatorial background events. The percentage of each background component in the Λ_b^0 signal region, computed from the Λ_b^0 mass fit, is $(89.5 \pm 1.7)\%$ Λ_b^0 baryons, $(7.2 \pm 0.6)\%$ B mesons, and $(3.3 \pm 0.1)\%$ combinatorial events. Other backgrounds such as 5-track decays of B^+ mesons are negligible, as confirmed in inclusive single b hadron simulations [16, 17]. The high mass region above the $\Lambda_b^0 \to \Lambda_c^+\pi^-$ signal in Fig. 1 determines the combinatorial background. Reconstructing $\bar{B}^0 \to D^+\pi^-$ data as $\Lambda_b^0 \to \Lambda_c^+\pi^-$ gives the B hadronization background. The Λ_b^0 hadronization background is obtained from a $\Lambda_b^0 \to \Lambda_c^+\pi^-$ PYTHIA simulation. The events in this simulation are reweighted so that the $p_{\rm T}(\Lambda_b^0)$ distribution agrees with data. As the simulation has fewer low momentum tracks around the Λ_b^0 than found in data, the simulated events are fur-

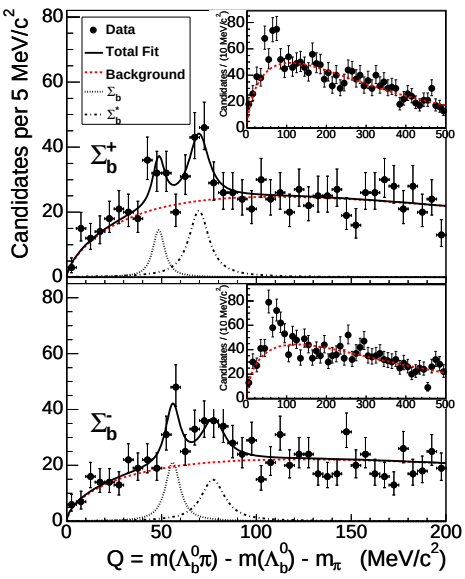

FIG. 2: The $\Sigma_b^{(*)}$ fit to the $\Lambda_b^0\pi^+$ and $\Lambda_b^0\pi^-$ subsamples. The top plot shows the $\Lambda_b^0\pi^+$ subsample, which contains $\Sigma_b^{(*)+}$, while the bottom plot shows the $\Lambda_b^0\pi^-$ subsample, which contains $\Sigma_b^{(*)-}$. The insets show the expected background plotted on the data for $Q \in [0,\ 500]$ MeV/c^2, while the signal fit is shown on a reduced range of $Q \in [0,\ 200]$ MeV/c^2.

ther reweighted until the $p_{\rm T}$ spectrum of tracks around the Λ_b^0 is consistent with data. After establishing the shape and normalization of each background Q distribution, the background shapes are parameterized by a power law multiplied by an exponential. The total background shape shown in Fig. 2 (inset) is compatible with the Q sidebands and is a fixed component in the $\Sigma_b^{(*)}$ fit.

In the Q signal region we observe an excess of events over the total background as shown in Fig. 2. The excess in the $\Lambda_b^0\pi^-$ subsample is 118 over 288 expected background candidates. In the $\Lambda_b^0\pi^+$ subsample the excess is 91 over 313 expected background candidates.

We perform a simultaneous unbinned maximum likelihood fit to the $\Lambda_b^0\pi^-$ and $\Lambda_b^0\pi^+$ subsamples for a signal from each expected $\Sigma_b^{(*)}$ state plus the background, referred to as the "four signal hypothesis." Each signal consists of a Breit-Wigner distribution convoluted with two Gaussian distributions describing the detector resolution, with a dominant narrow core and a small broad component for the tails. The natural width of each Breit-Wigner distribution is computed from the central Q value [8]. The expected difference of the isospin mass splittings within the Σ_b^* and Σ_b multiplets is below our sensitivity with this sample of data. Consequently, we constrain $m(\Sigma_b^{*+}) - m(\Sigma_b^+) = m(\Sigma_b^{*-}) - m(\Sigma_b^-) \equiv \Delta_{\Sigma_b^*}$. The four Σ_b signal fit to data, which has a fit probability of 76% in the range $Q \in [0, 200]$ MeV/c^2, is shown in Fig. 2.

Systematic uncertainties on the mass difference and yield measurements fall into three categories: mass scale, $\Sigma_b^{(*)}$ background model, and $\Sigma_b^{(*)}$ signal parameterization. The systematic uncertainty on the mass scale is determined by the discrepancies of the CDF II measured masses of the D^*, Σ_c, and Λ_c^* hadrons from the world average mass values [15]. The Q value dependence of this systematic uncertainty is modeled with a linear function, which is used to extrapolate the mass scale uncertainty for each $\Sigma_b^{(*)}$ Q value. This is the largest systematic uncertainty for the mass difference measurements, ranging from 0.1 to 0.3 MeV/c^2. The systematic effects related to assumptions made on the $\Sigma_b^{(*)}$ background model are: the sample composition of the Λ_b^0 signal region, the normalization and functional form of the Λ_b^0 hadronization background taken from a PYTHIA simulation, and our limited knowledge of the shape of the Λ_b^0 hadronization background (the largest systematic uncertainty on the yield measurements, ranging from 2 to 15 events). The systematic effects related to assumptions made on the $\Sigma_b^{(*)}$ signal parameterization are: underestimation of the detector resolution, the uncertainty in the natural width prediction from [8], and the constraint that $m(\Sigma_b^{*+}) - m(\Sigma_b^+) = m(\Sigma_b^{*-}) - m(\Sigma_b^-)$.

The significance of the signal is evaluated using the likelihood ratio, $LR \equiv L/L_{\rm alt}$, where L is the likelihood of the four signal hypothesis and $L_{\rm alt}$ is the likelihood of an alternative hypothesis [21]. We study the alternate hypotheses of no signal, two Σ_b states (one per $\Lambda_b^0\pi$ charge combination), and three $\Sigma_b^{(*)}$ states, performed by eliminating one of the states in the four signal hypothesis. Systematic variations are included in the fit as nuisance parameters over which the likelihood is integrated. The resulting likelihood ratios are given in Tab. I. To assess the significance of the signal, we repeat the four signal hypothesis fit on samples randomly generated from alternate signal hypotheses. In 12 million background samples, none had a LR equivalent or greater than the one found in data. We evaluate the probability for background only to produce four signals of this or greater significance to be less than 8.3×10^{-8}, corresponding to a significance of greater than 5.2 σ. The probabilities for each of the alternate hypotheses to produce the observed signal structure is also given in Tab. I. The final results for the Σ_b measurement are quoted in Tab. II. Using the CDF II measurement of $m_{\Lambda_b^0} = 5619.7 \pm 1.2$ (stat.) ± 1.2 (syst.) MeV/c^2 [22], we find the absolute masses of the Σ_b states given in Tab. II. The systematic uncertainties on the absolute Σ_b mass values are dominated by the total Λ_b^0 mass uncertainty.

In summary, using a sample of 3180 ± 60 (stat.) $\Lambda_b^0 \to \Lambda_c^+\pi^-$ candidates reconstructed in 1.1 fb^{-1} of CDF II data, we search for resonant $\Lambda_b^0\pi^\pm$ states. We observe a signal of four states whose masses and widths are consistent with those expected for the lowest-lying charged $\Sigma_b^{(*)}$ baryons. This result represents the first observation

Hypothesis	LR	p-value	Significance (σ)
No Signal	2.6×10^{18}	$< 8.3 \times 10^{-8}$	> 5.2
Two Σ_b States	4.4×10^{6}	9.2×10^{-5}	3.7
No Σ_b^- Signal	1.2×10^{5}	3.2×10^{-4}	3.4
No Σ_b^+ Signal	49	9.0×10^{-3}	2.4
No Σ_b^{*-} Signal	4.9×10^{4}	6.4×10^{-4}	3.2
No Σ_b^{*+} Signal	8.1×10^{4}	6.0×10^{-4}	3.2

TABLE I: Likelihood ratios (LR) in favor of the four signal hypothesis over alternative hypotheses. Also shown is the probability for each hypothesis to produce the observed data (p-value), calculated using the LR as a test statistic on randomly generated samples. The final column gives the equivalent standard deviations from the normal distribution.

State	Yield	Q or $\Delta_{\Sigma_b^*}$ (MeV/c^2)	Mass (MeV/c^2)
Σ_b^+	32^{+13+5}_{-12-3}	$Q_{\Sigma_b^+} = 48.5^{+2.0+0.2}_{-2.2-0.3}$	$5807.8^{+2.0}_{-2.2} \pm 1.7$
Σ_b^-	59^{+15+9}_{-14-4}	$Q_{\Sigma_b^-} = 55.9 \pm 1.0 \pm 0.2$	$5815.2 \pm 1.0 \pm 1.7$
Σ_b^{*+}	77^{+17+10}_{-16-6}	$\Delta_{\Sigma_b^*} = 21.2^{+2.0+0.4}_{-1.9-0.3}$	$5829.0^{+1.6+1.7}_{-1.8-1.8}$
Σ_b^{*-}	69^{+18+16}_{-17-5}		$5836.4 \pm 2.0^{+1.8}_{-1.7}$

TABLE II: Final results for the Σ_b measurement. The first uncertainty is statistical and the second is systematic. The absolute Σ_b mass values are calculated using a CDF II measurement of the Λ_b^0 mass [22], which contributes to the systematic uncertainty.

of the $\Sigma_b^{(*)}$ baryons.

We thank T. Becher, A. Falk, D. Pirjol, J. Rosner, and D. Ebert for useful discussions. We also thank the Fermilab staff and the technical staffs of the participating institutions for their vital contributions. This work was supported by the U.S. Department of Energy and National Science Foundation; the Italian Istituto Nazionale di Fisica Nucleare; the Ministry of Education, Culture, Sports, Science and Technology of Japan; the Natural Sciences and Engineering Research Council of Canada; the National Science Council of the Republic of China; the Swiss National Science Foundation; the A.P. Sloan Foundation; the Bundesministerium für Bildung und Forschung, Germany; the Korean Science and Engineering Foundation and the Korean Research Foundation; the Particle Physics and Astronomy Research Council and the Royal Society, UK; the Institut National de Physique Nucleaire et Physique des Particules/CNRS; the Russian Foundation for Basic Research; the Comisión Interministerial de Ciencia y Tecnología, Spain; the European Community's Human Potential Programme under contract HPRN-CT-2002-00292; and the Academy of Finland.

[1] A. V. Manohar and M. B. Wise, Phys. Rev. D **49**, 1310 (1994).

[2] D. P. Stanley and D. Robson, Phys. Rev. Lett. **45**, 235 (1980). D. P. Stanley and D. Robson, Phys. Rev. D **21**, 3180 (1980). D. Izatt, C. DeTar, and M. Stephenson, Nucl. Phys. **B199**, 269 (1982). J. M. Richard and P. Taxil, Phys. Lett. B **128**, 453 (1983). J. L. Basdevant and S. Boukraa, Z. Phys. C **30**, 103 (1986). W. Y. P. Hwang and D. B. Lichtenberg, Phys. Rev. D **35**, 3526 (1987). A. Martin and J. M. Richard, Phys. Lett. B **185**, 426 (1987). D. B. Lichtenberg, R. Roncaglia, J. G. Wills, and E. Predazzi, Z. Phys. C **47**, 83 (1990).

[3] E. Jenkins, Phys. Rev. D **54**, 4515 (1996). E. Jenkins, Phys. Rev. D **55**, 10 (1997).

[4] C. Albertus, J. E. Amaro, E. Hernandez, and J. Nieves, Nucl. Phys. **A740**, 333 (2004). D. Ebert, R. N. Faustov, and V. O. Galkin, Phys. Rev. D **72**, 034026 (2005). S. Capstick, Phys. Rev. D **36**, 2800 (1987).

[5] R. Roncaglia, D. B. Lichtenberg, and E. Predazzi, Phys. Rev. D **52**, 1722 (1995). M. Karliner and H. J. Lipkin, hep-ph/0307243; condensed version in Phys. Lett. B **575**, 249 (2003).

[6] K. C. Bowler *et al.* (UKQCD Collaboration), Phys. Rev. D **54**, 3619 (1996). N. Mathur, R. Lewis, and R. M. Woloshyn, Phys. Rev. D **66**, 014502 (2002).

[7] J. L. Rosner, Phys. Rev. D **57**, 4310 (1998). J. L. Rosner, Phys. Rev. D **75**, 013009 (2007).

[8] J. G. Körner, M. Krämer, and D. Pirjol, Prog. Part. Nucl. Phys. **33**, 787 (1994).

[9] D. Acosta *et al.* (CDF Collaboration), Phys. Rev. D **71**, 032001 (2005).

[10] A. Sill *et al.*, Nucl. Instrum. Methods A **447**, 1 (2000).

[11] A. Affolder *et al.* (CDF Collaboration), Nucl. Instrum. Methods A **526**, 249 (2004).

[12] W. Ashmanskas *et al.* (CDF Collaboration), Nucl. Instrum. Methods A **518**, 532 (2004).

[13] E. J. Thomson *et al.*, IEEE Trans. Nucl. Sci. **49**, 1063 (2003).

[14] The transverse plane (x, y) is perpendicular to the direction of the proton beam. The azimuthal angle ϕ is measured from the x-axis. The transverse momentum $p_{\rm T}$ is the magnitude of the projection of the momentum in the transverse plane.

[15] W. M. Yao *et al.* (Particle Data Group), J. Phys. G **33**, 1 (2006).

[16] We use a variety of single b hadron simulations, all using the $p_{\rm T}(B)$ and $y(B)$ distributions obtained from B decays in data (D. Acosta *et al.* (CDF Collaboration), Phys. Rev. D **71**, 032001 (2005)). The simulated $p_{\rm T}(\Lambda_b^0)$ distribution is reweighted to match the sideband-subtracted data.

[17] The b hadrons are decayed using the EvtGen package, D. J. Lange, Nucl. Instrum. Methods A **462**, 152 (2001).

[18] A. Abulencia *et al.* (CDF Collaboration), Phys. Rev. Lett. **98**, 122002 (2007).

[19] A. K. Leibovich and I. W. Stewart, Phys. Rev. D **57**, 5620 (1998).

[20] T. Sjöstrand, P. Eden, C. Friberg, L. Lonnblad, G. Miu, S. Mrenna, and E. Norrbin, Comput. Phys. Commun. **135**, 238 (2001).

[21] R. Royall, J. Amer. Statist. Assoc. **95**, 760 (2000).

[22] D. Acosta *et al.* (CDF Collaboration), Phys. Rev. Lett. **96**, 202001 (2006).